

Frequency-independent breakdown strength of dielectric elastomers under AC stress

Iannarelli, A.; Ghaffarian Niasar, M.; Ross, Rob

DOI

[10.1063/1.5115473](https://doi.org/10.1063/1.5115473)

Publication date

2019

Document Version

Accepted author manuscript

Published in

Applied Physics Letters

Citation (APA)

Iannarelli, A., Ghaffarian Niasar, M., & Ross, R. (2019). Frequency-independent breakdown strength of dielectric elastomers under AC stress. *Applied Physics Letters*, 115(9), 092904-1 - 092904-5. Article 092904. <https://doi.org/10.1063/1.5115473>

Important note

To cite this publication, please use the final published version (if applicable). Please check the document version above.

Copyright

Other than for strictly personal use, it is not permitted to download, forward or distribute the text or part of it, without the consent of the author(s) and/or copyright holder(s), unless the work is under an open content license such as Creative Commons.

Takedown policy

Please contact us and provide details if you believe this document breaches copyrights. We will remove access to the work immediately and investigate your claim.

Frequency-independent breakdown strength of dielectric elastomers under AC stress

A. Iannarelli,^{1, a)} M. Ghaffarian Niasar,¹ and Rob Ross¹

Electrical sustainable energy department, Delft University of Technology, Delft, 2628CD The Netherlands.

(Dated: 13 August 2019)

Soft insulators are the main component used in dielectric elastomer actuators (DEAs). It follows that dielectric properties like permittivity and dielectric strength of the insulator can strongly influence the maximum dynamic actuation performance of DEA devices. We observed an increasing breakdown voltage with increasing driving AC voltage frequency for silicone-based dielectric films. Despite the breakdown voltage increase, we demonstrate that there is no actual breakdown electric field rise with varying frequency. We show that the voltage behavior is rather compatible with a constant dielectric breakdown field model and the slow mechanical response of the elastomer.

Dielectric elastomers have been intensely studied in recent years as they are the key component to manufacture soft, lightweight, and noiseless electrostatic transducers¹. A dielectric elastomer actuator (DEA) consists of a thin layer of dielectric and elastic polymer sandwiched between a pair of compliant electrodes. By applying an adequate electric potential difference, the dielectric contracts under the electrodes electrostatic pressure, causing a displacement along the compression direction. The energy density stored in this action is proportional to the square of the input voltage. It follows that the best performance of the system are obtained maximizing the applied voltage without occurring in electrical breakdown failure.

The dielectric strength of the insulating layer is a crucial property of the elastomer used for DEA. This is the maximum allowed electric field that the dielectric elastomer can withstand without electrically break down. As a consequence, it establishes the performances boundary of the DEA². Knowing this property is a crucial point to design better and outperforming actuators. From high-voltage technology³, it is long known that the electric breakdown strength of dielectric materials can vary from AC to DC voltages and the amount of change depends on the frequency considered.

For polymers, lower breakdown field strength is generally observed in AC electric stress case compared with DC⁴. This trend can have negative impact also on the DEAs since they are intended to work with dynamical electrical stresses, i.e. AC voltages. For this reason, we expect a breakdown voltage reduction of the insulator and, consequently, a general lowering in the actuator performances. Despite its relevance, the AC breakdown voltage of commonly used dielectric elastomers has been, at date, scarcely studied⁵.

In the present contribution, we show that the AC breakdown voltage of silicone-based dielectric elastomer actuators actually increases with the frequency, in contrast to what is usually experienced for other thin film polymers⁶. However, rather than a true dielectric strength improvement, we found that this phenomenon results from the viscoelastic nature of the insulator.

We measured the frequency-dependent breakdown voltage of samples prepared with Elastosil 2030-100, which is

a common silicone dielectric elastomer (Polydimethylsiloxane, PDMS) used in DEA manufacture. The samples were cut from PDMS sheets into 50 mm diameter disks and divided in two sets with different mechanical constraints. The first set was prepared applying a permanent biaxial pre-stretch using an in-house built circular stretching rig⁷. A radial extension of $\lambda = 1.5$ times the initial radius was chosen. To hold the imposed mechanical tension, the membranes were successively clamped to ring-shaped PMMA frames. The second set

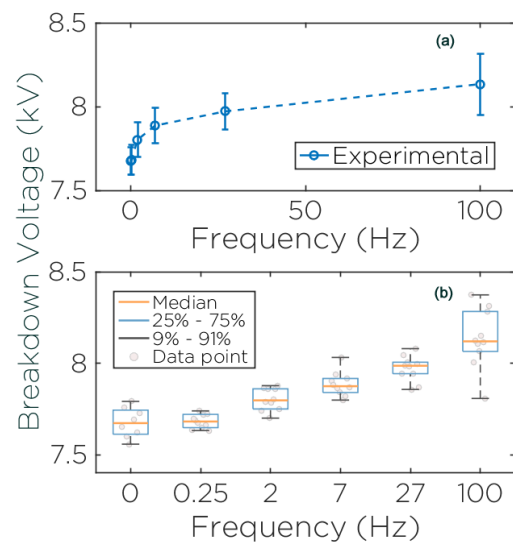


FIG. 1. (a) Increasing average breakdown voltages resulting from the AC tests for the pre-stretched membranes. In (b) the dispersion of the actual measurements.

was prepared with no pre-stretch, and the corresponding disks were directly fastened to the frames. Subsequently, compliant circular electrodes (12 mm diameter) were spray-painted on both membrane sides using a conductive mixture of carbon black and PDMS⁸. Lastly, contacts were added using carbon grease and silver-paint pads.

The AC breakdown voltage is measured as follows: the amplitude of a positive-clamped sine wave is linearly increased at a constant rate v until dielectric failure of the sample occurs. The highest registered voltage right before the irreversible failure, is referred as breakdown voltage. The AC frequen-

^{a)}Electronic mail: a.iannarelli@tudelft.nl

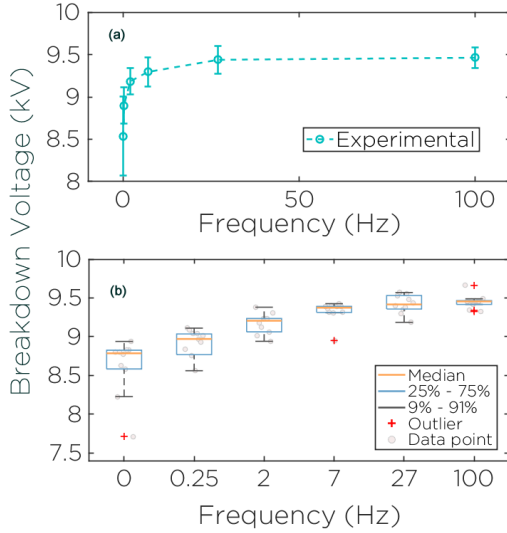


FIG. 2. (a) Average breakdown voltages at various frequencies for the non-stretched membranes. In (b) the statistical spread of the data points is shown.

cies used are in the range $\mathcal{F} = \{0(DC), 0.25, 2, 7, 27, 100\}$ Hz, and are logarithmically spaced between 2 and 100 Hz. The linear increase rate $v = 8 \frac{V}{s}$, is the same in all the tests. For each frequency in \mathcal{F} ten different samples are tested⁹.

According to the reported experimental data, Fig.1-2, there is a steady increase in the breakdown voltage with the frequency. The non-stretched samples, exhibit the most pronounced relative voltage change from DC to 100 Hz (around 11%) while for the pre-stretched membranes the variation is less than 4%.

To understand the nature of these results, we explored the system's electrical and mechanical contributions to the breakdown, separately.

From an electrical point of view, the high resistivity of the carbon-silicone electrodes builds up with the sample's capacitance a distributed RC network. This causes a non-homogeneous spatial voltage-distribution on the electrodes¹⁰. Accordingly, the voltage across the active area is lower than the initial AC input. To compensate this potential drop and have a sufficiently large voltage to trigger the breakdown, a higher input voltage is thus required at higher frequencies. We verified this mechanism by performing dielectric spectroscopy measurements on our DEAs. An insulation analyzer (Megger Idax 300) is used to measure the real capacitance of the samples over a broad frequency range (10 mHz to 10 kHz) at low and high voltage. If the active surface reduces or the voltage drops due to the frequency, the effect is visible as a capacitance variation within the frequency range \mathcal{F} ¹¹. Fig.3 shows that no significant capacitance alteration is observed in both membranes sets for frequencies up to 1 kHz. Only a small change (less than 1%) is recorded from 100 mHz to 1 kHz when performing tests with high voltage (1400 V_{rms}). The DEA is electrically reactive and allows the full voltage on the active area during the AC cycle.

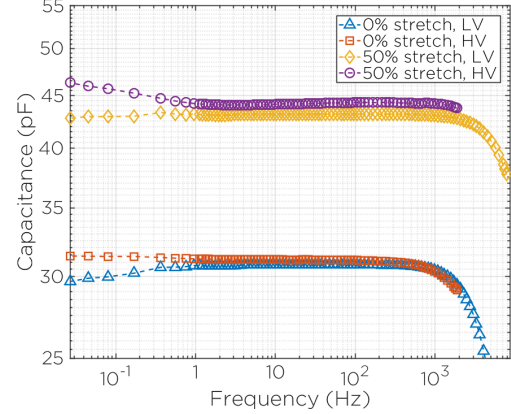


FIG. 3. Capacitance measurement for non-stretched and pre-stretched membranes at low (LV=7 V_{rms}) and high voltage (HV=1400 V_{rms}).

As a further confirmation, we computed the finite element model of our DEA using COMSOL software. For the simulation we used the relative permittivity $\epsilon_r = 2.7$ for the membrane and conductivity $\sigma = 0.82 \frac{S}{m}$ for the electrodes. This value was measured using a four-point-probe configuration on the real sample under low voltage condition (5 V). From the computed model (Fig.4), it is found that the voltage starts to drop at the center of the active area for frequencies above 2 kHz. This simulation confirms that the voltage is uniformly distributed on the electrodes in the range \mathcal{F} , Figure 4(d).

The combined results from dielectric spectroscopy and finite element modeling suggest that, at least in the range \mathcal{F} , the capacitor-like system has an unaltered electrical response. We can, therefore, exclude the limited conductivity of the electrodes as the cause of breakdown voltage increase. We finally explored the mechanical contribution to the breakdown voltage variation by investigating the rheology of the silicone film under periodic compression stresses. The sample compression was measured using a laser vibrometer (Polytec OFV-5000) with the setup schematized in Fig.5. This configuration measures the single-sided relative displacement of the electrode surface with respect to the laser-head down to 2 nm resolution. To guarantee reliable displacement measurements in the compression direction, the laser beam was accurately aligned with each geometrical sample center. This reduces the possibility of measurement drifts coming from the sample lateral expansion during compression. The electrodes surface reflectance was improved by sputtering a thin gold layer (approximately 25 nm) on them.

The mechanical compression was induced by applying high voltage AC to the DEAs. The peak-to-peak amplitude was fixed to $V_{50}=2$ kV in case of the pre-stretched samples, and $V_0=4$ kV for the rest. The data are collected in the range from 50 mHz to 500 Hz. For each frequency the displacement-amplitude is estimated over a minimum of 200 cycles.

Fig.6(a)-(b) show the resulting displacement amplitude as

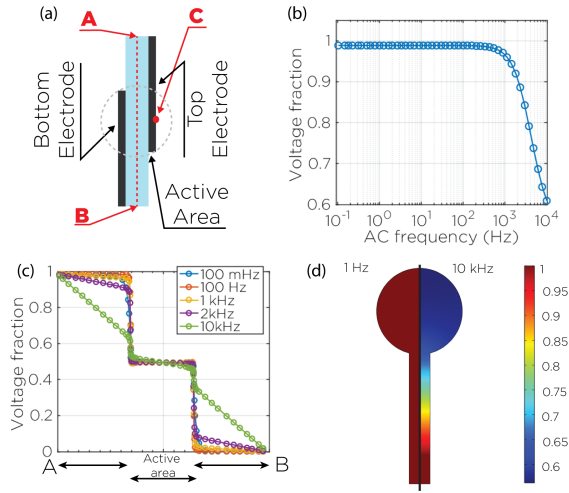


FIG. 4. Finite element method model: (a) Not-to-scale cross-section of the sample, showing the sectioning line (AB), the electrode center C and the active (overlapping) area; (b) Fraction of the applied voltage taken at point C ; (c) Voltage along AB ; (d) Voltage distribution on single-side spray electrode for low frequency (1 Hz) and high frequency (10 kHz)

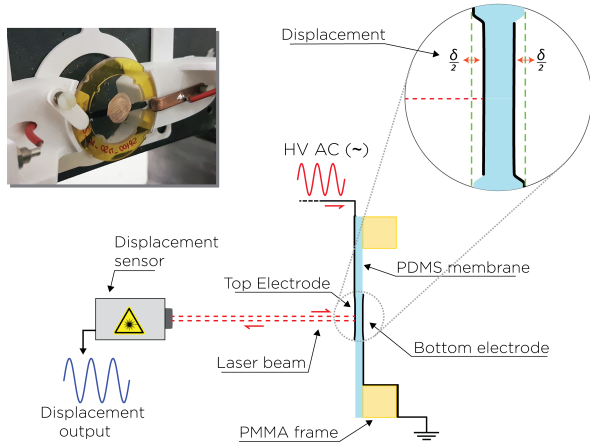


FIG. 5. Schematic overview of the displacement setup. In upper-left inset, the front-view of a real sample under test.

a function of the actuation frequency for both samples sets. Each curve has been averaged on measurements over 5 different samples. It can be noted that overestimated peaks are present in both graphs. This glitch happens in proximity of the membrane resonant frequency, which causes out-of-plane displacements¹². The specific choice of the \mathcal{F} range ensures that most of the frequency points fall before the first resonance peak and, as a result, reliable displacement measurements are available.

In both sets, the displacement dampens with increasing frequency in the range \mathcal{F} . The viscoelasticity of the samples, slows the dynamic compression and the elastomer cannot fully contract within an AC period¹³. As a consequence, for a given voltage amplitude, the resulting electric field is lower at higher frequencies because the material does not compress

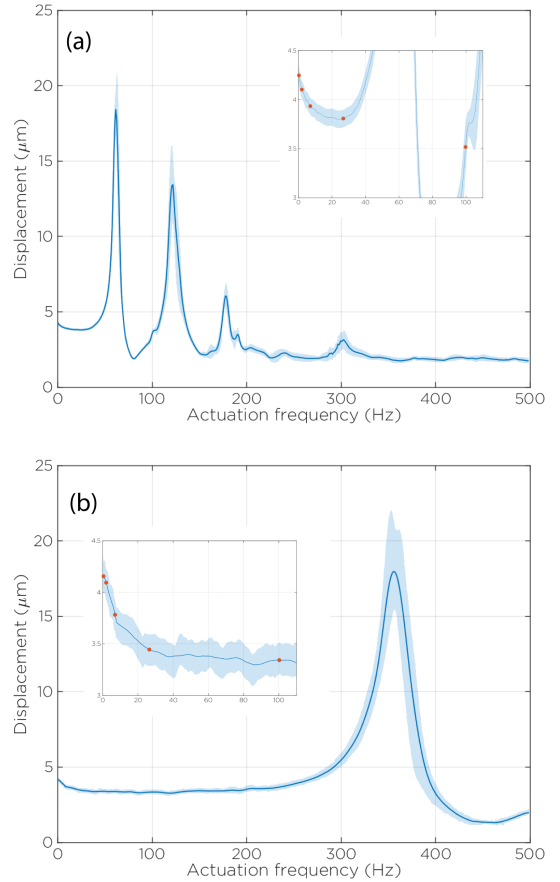


FIG. 6. Average displacement magnitude resulting from AC voltage over frequency measurement for (a) non-stretched and (b) pre-stretched samples. The light-blue shade indicates the measurements standard deviation. The insets show the studied range \mathcal{F} . The red dots correspond to the exact displacement values used in the calculations for our model.

enough and is therefore thicker.

Starting from the frequency-dependent displacement results, we show that the increasing breakdown voltage over frequency is actually compatible with a constant electric breakdown field model. In a very general manner, for a parallel plate capacitor-like system the breakdown voltage V_{BD} and the electric breakdown field E_{BD} are related by

$$V_{BD}(\omega) = E_{BD}(\omega, d_0) d_{final} = E_{BD}(\omega) [d_0 - \delta d(V, \omega)] \quad (1)$$

where d_{final} is the dielectric's thickness at breakdown. The breakdown strength $E_{BD}(\omega, d_0)$ also depends on the initial thickness, but for any given d_0 this value is known and constant¹⁴. The final thickness is rewritten as the difference of the initial thickness d_0 and the displacement $\delta d(V, \omega)$ caused by the electrostatic force, which is dependent on the voltage frequency ω and its amplitude V . We write the displacement δd as the product:

$$\delta d = \alpha(V) g(\omega) \quad (2)$$

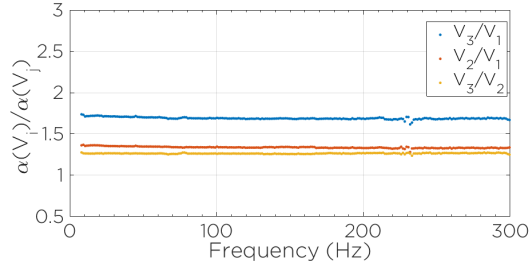


FIG. 7. Ratios of displacements measured at various driving voltages ($V_1=1.5$ kV, $V_2=1.75$ kV, $V_3=2$ kV) as a function of frequency for the pre-stretched sample case.

where $\alpha(V)$ is the displacement that the membrane would undergo at equilibrium with the DC voltage V and $g(\omega)$ is a frequency attenuation factor, that takes into account the material viscoelastic response to the frequency.

The assumption in (2) was empirically proved to be valid in the range \mathcal{F} by measuring different ratios $\frac{\delta d(V_i, \omega)}{\delta d(V_j, \omega)} = \frac{\alpha(V_i)}{\alpha(V_j)}$ for various voltages V_i, V_j . The ratios turned out to be constant regardless the frequency ω , see Fig 7.

We now make the assumption of a constant electric breakdown field $E_{BD}(\omega) = E_{BD}, \forall \omega \in \Omega = 2\pi\mathcal{F}$ and we compare the breakdown field at any frequency with the reference frequency $\omega_0 = 0$, that corresponds to the DC case. Using (2) in (1) we have

$$\begin{aligned} V_{BD}(\omega) - V_{BD}(0) &= E_{BD}[\delta d(V_{BD}, 0) - \delta d(V_{BD}, \omega)] \\ &= E_{BD}\alpha(V_{BD})[g(0) - g(\omega)] \end{aligned} \quad (3)$$

For practical reasons, we are unable to measure the final compression $\delta(V_{BD}, \omega)$ at breakdown voltage V_{BD} . This is because for extreme displacement the membrane can wrinkle or be sampled out of plane, giving erroneous results. As a workaround, we measured the displacement $\delta d_1(V_1, \omega)$ at a lower value $V_1 \ll V_{BD}$ and we exploit the property of (2) by replacing it into (3). We finally obtain

$$V_{BD}(\omega) - V_{BD}(0) = \kappa[\delta d(V_1, 0) - \delta d(V_1, \omega)] \quad (4)$$

the quantity $\kappa = E_{BD} \frac{\alpha(V_{BD})}{\alpha(V_1)}$ only depends on voltage amplitudes and breakdown field, and is thus, by previous hypothesis, constant. Equation (4) states that, assuming a constant electric breakdown field independent from the frequency, the difference between any breakdown voltage with a reference value is proportional to the respective compression-displacements difference. The constant κ depends on the dielectric strength of the material and the voltage-displacement relation. Note that for the proposed model it is not important to know the exact value of E_{BD} (which remains unknown) but rather the assumption of it being constant.

We combined the results from compression tests and breakdown voltage measurements using Equation (4) for both non-stretched and stretched samples cases. Fig.8 shows that the relative-to-DC breakdown voltages and the related displacements actually follow the trend described by the proposed

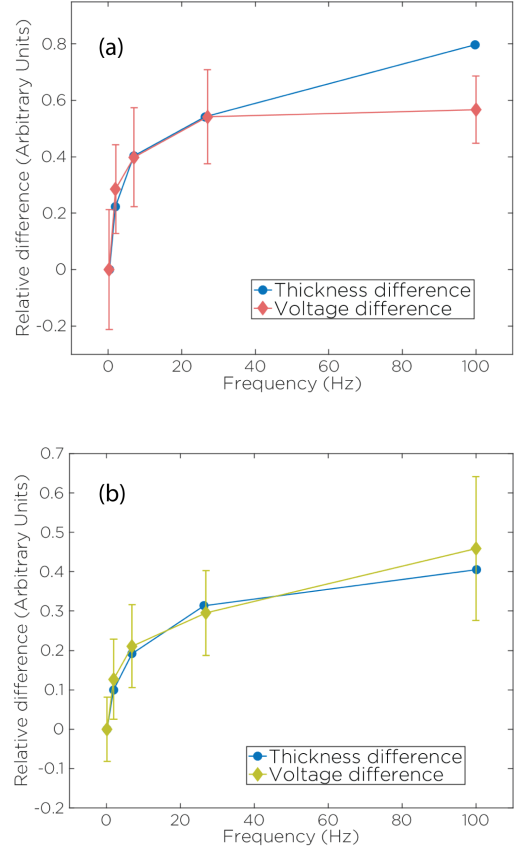


FIG. 8. Comparison of voltage amplitude difference with displacement difference for (a) non-stretched and (b) pre-stretched samples in the range of frequency considered.

model in Equation (4). The constant of proportionality was empirically calculated to best fit the results and equals $\kappa_0=1058$ kV/mm for the non-stretched case and $\kappa_{50}=266$ kV/mm for the stretched case. Although these quantities have the unit of an electric field, they must not be confused with the relative dielectric strength E_{BD} from which they differ by a constant. The point relative to 100 Hz for the non-stretched samples lies outside the trend. Because this is sampled near an out-of-plane resonance, we consider it as an outlier, Fig. (6)(a). There is a good agreement between the proposed model and the experimental data for both the cases examined. Moreover, it is also able to justify the lower change in breakdown voltage for the pre-stretched membranes. The pre-tensioning improves the elastomer rheology making it react faster to the compressive force¹⁵.

In conclusion, we experimentally found that the increase of the breakdown voltage with increasing frequency is not caused by the limited electrodes conductivity at high frequency nor to improved permittivity. The phenomenon is rather justified with the viscoelastic reaction of the silicone membrane. The apparent dielectric strength improvement that could result from a non-correct interpretation of the breakdown voltages cannot be in any way exploited to enhance the

performance of the DEA. The electric field at breakdown is constant and does not depend on the frequency used in the investigated range. The breakdown voltage increase is explained by a less effective elastic compression at higher frequency. We proved this hypothesis by proposing an empirical model for the frequency-dependent displacement that accurately reproduces this behavior in the frequency range of interest. We proved this hypothesis by proposing an empirical model for the frequency-dependent displacement which accurately reproduces this behavior in the frequency range of interest. To focus on essential ideas, we have restricted the materials choice as well as the electrodes geometry. The model can, however, be extended to other samples geometry and further materials.

¹S. Rosset and H. Shea, "Small, fast, and tough: Shrinking down integrated elastomer transducers," *Applied Physics Reviews* **3**, 031105 (2016).

²R. Kornbluh, A. Wong-Foy, R. Pelrine, H. Prahlad, and B. McCoy, "Long-lifetime all-polymer artificial muscle transducers," *MRS Proceedings* **1271**, 1271JJ03-01 (2010).

³L. A. Dissado and J. C. Fothergill, *Electrical Degradation and Breakdown in Polymers* (IET, 1992).

⁴A. Laifaoui, M. S. Herzine, Y. Zebboudj, J.-M. Reboul, and M. Nedjar, "Breakdown strength measurements on cylindrical polyvinyl chloride sheaths under ac and dc voltages," *IEEE Transactions on Dielectrics and Electrical Insulation* **21**, 2267-2273 (2014).

⁵M. Yamada, Y. Murakami, T. Kawashima, and M. Nagao, "Electrical

breakdown of dielectric elastomer and its lamination effect," in *2014 IEEE Conference on Electrical Insulation and Dielectric Phenomena (CEIDP)*.

⁶K. Miyairi, "The frequency dependent dielectric breakdown in some thin film polymers," *Proceedings of the 7th International Conference on Properties and Applications of Dielectric Materials* (2003).

⁷S. E. Schausberger, R. Kaltseis, M. Drak, U. Cakmak, Z. Major, and S. Bauer, "Cost-efficient open source desktop size radial stretching system with force sensor," *IEEE Access* **3**, 556-561 (2015).

⁸S. Rosset, O. A. Araromi, S. Schlatter, and H. R. Shea, "Fabrication process of silicone-based dielectric elastomer actuators," *Journal of Visualized Experiments* **108**, 53423 (2016).

⁹F. Carpi, I. Anderson, S. Bauer, G. Frediani, G. Gallone, M. Gei, C. Graaf, C. Jean-Mistral, W. Kaal, G. Kofod, M. Kollosche, R. Kornbluh, B. Lassen, M. Matysek, S. Michel, S. Nowak, B. O'Brien, Q. Pei, R. Pelrine, B. Rechenbach, S. Rosset, and H. Shea, "Standards for dielectric elastomer transducers," *Smart Materials and Structures* **24**, 105025 (2015).

¹⁰E. M. Henke, K. E. Wilson, and I. A. Anderson, "Modeling of dielectric elastomer oscillators for soft biomimetic applications," *Bioinspiration & Biomimetics* **13**, 046009 (2018).

¹¹H. Stoyanov, D. Mc Carthy, M. Kollosche, and G. Kofod, "Dielectric properties and electric breakdown strength of a supercolative composite of carbon black in thermoplastic copolymer," *Applied Physics Letters* **94**, 232905 (2009).

¹²C. Tang, B. Li, Z. Li, C. Bian, L. Liu, and H. Chen, "Dynamic characteristics of out-of-plane vibration of dielectric elastomer resonator," (2018).

¹³W. Hong, "Modeling viscoelastic dielectrics," *Journal of the Mechanics and Physics of Solids* **59**, 637 - 650 (2011).

¹⁴D. Gatti, H. Haus, M. Matysek, B. Frohnappel, C. Tropea, and H. F. Schlaak, "The dielectric breakdown limit of silicone dielectric elastomer actuators," *Applied Physics letters* **104**, 052905 (2014).

¹⁵J. Huang, S. Shian, R. M. Diebold, Z. Suo, and D. R. Clarke, "The thickness and stretch dependence of the electrical breakdown strength of an acrylic dielectric elastomer," *Applied Physics Letters* **101**, 122905 (2012).